

Lecture 3 : Time Effects Observed in Granular Materials

Kenichi Soga, University of Cambridge

3-1 Engineering Properties of Granular Soils

Virtually every soil "lives" in that all of its properties undergo changes with time - some insignificant, but others very important. Time-dependent chemical, geomicrobiological, and mechanical processes may result in compositional and structural changes that lead to softening, stiffening, strength loss, strength gain, or altered conductivity properties. The need to predict what the properties and behavior will be months to hundreds or thousands of years from now based on what we know today is a major challenge in geoen지니어ing.

When soil is subjected to a constant load, it deforms over time and this is usually called creep. The inverse phenomenon, usually termed stress relaxation, is a drop in stress over time after a soil is subjected to a particular constant strain level. Creep and relaxation are two consequences of the same phenomenon; i.e. time-dependent changes in structure. The rate and magnitude of these time-dependent deformations are determined by these changes.

Time-dependent deformations and stress relaxation are important in geotechnical problems wherein long-term behavior is of interest. These include long-term settlement of structures on compressible ground, deformations of earth structures, movements of natural and excavated slopes, squeezing of soft ground around tunnels, and time- and stress-dependent changes in soil properties. The time-dependent deformation response of a soil may assume a variety of forms owing to the complex interplays among soil structure, stress history, drainage conditions, and changes in temperature, pressure, and bio-chemical environment with time. Time-dependent deformations and stress relaxations usually follow logical and often predictable patterns, at least for simple stress and deformation states such as uniaxial and triaxial compression.

Time-dependent deformation and stress phenomena in soils are important not only because of the immediate direct application of the results to analyses of practical problems, but also because the results can be used to obtain fundamental information about soil structure, interparticle bonding, and the mechanisms controlling the strength and deformation behavior. Both micro-scale and macro-scale phenomena are discussed because understanding of micro-scale processes can provide a rational basis for prediction of macro-scale responses.

3-2 General Characteristics

1. Soils exhibit both *creep* and *stress relaxation*, Fig. 3.1. *Creep* is the development of time-dependent shear and/or volumetric strains that proceed at a rate controlled by the viscous-like resistance of soil structure. *Stress relaxation* is a time-dependent decrease in stress at constant deformation. The relationship between creep strain and the logarithm of time may be linear, concave upward, or concave downward as shown by the examples in Fig. 3.2. The term creep is used herein to refer to time-dependent shear strains and/or volumetric strains that develop at a rate controlled by the viscous resistance of the soil structure. Secondary compression refers to the special case of volumetric strain that follows primary consolidation. The rate of secondary compression is controlled by the

viscous resistance of the soil structure, whereas, the rate of primary consolidation is controlled by hydrodynamic lag; i.e., how fast water can escape from the soil.

2. The magnitude of these effects increases with increasing plasticity, activity, and water content of the soil. The most active clays usually exhibit the greatest time-dependent responses (i.e. smectite > illite > kaolinite). This is because the smaller the particle size, the greater is the specific surface, and the greater the water adsorption. Thus, under a given consolidation stress or deviatoric stress, the more active and plastic clays (smectites) will be at higher water content and lower density than the inactive clays (kaolinites). Normally consolidated soils exhibit larger magnitude of creep than overconsolidated soils. However, the basic form of behavior is essentially the same for all soils; i.e. undisturbed and remolded clay, wet clay, dry clay, normally and overconsolidated soil, and wet and dry sand.
3. An increase in deviatoric stress level results in an increased rate of creep as shown in Fig. 3.1. Some soils may fail under a sustained creep stress significantly less (as little as 50 percent) than the peak stress measured in a shear test, wherein a sample is loaded to failure in a few minutes or hours. This is termed *creep rupture*, and an early illustration of its importance was the development of slope failures in the Cucaracha clay shale, which began some years after the excavation of the Panama Canal (Casagrande and Wilson, 1951).
4. The creep response shown by the upper curve in Fig. 3.1 is often divided into three stages. Following application of a stress there is first a period of transient creep during which the strain rate decreases with time, followed by creep at nearly a constant rate for some period. For materials susceptible to creep rupture, the creep rate then accelerates leading to failure. These three stages are termed primary, secondary, and tertiary creep.
5. An example of strain rates as a function of stress for undrained creep of remolded illite is shown in Fig. 3.3. At low deviator stress, creep rates are very small and of little practical importance. At deviator stress approaching the strength of the material, the strain rates become very large and signal the onset of failure.
6. A characteristic relationship between strain rate and time exists for most soils, as shown, for example, in Fig. 3.4 for drained triaxial compression creep of London clay (Bishop, 1966) and Fig. 3.5 for undrained triaxial compression creep of soft Osaka clay (Murayama and Shibata, 1958). At any stress level (shown as a percentage of the strength before creep in Fig. 3.4 and in kg/cm^2 in Fig. 3.5), the logarithm of the strain rate decreases linearly with increase in the logarithm of time. The slope of this relationship is essentially independent of the creep stress; increases in stress level shift the line vertically upward. The slope of the log strain rate vs. log time line for drained creep is approximately -1. Undrained creep often results in a slope between -0.8 and -1 for this relationship. The onset of failure under higher stresses is signaled by a reversal in slope, as shown by the topmost curve in Fig. 3.5.
7. Pore pressure may increase, decrease, or remain constant during creep, depending on the volume change tendencies of the soil structure and whether or not drainage occurs during the deformation process. In general, saturated soft sensitive clays

under undrained conditions are most susceptible to strength loss during creep due to reduction in effective stress caused by increase in pore water pressure with time. Heavily overconsolidated clays under drained conditions are also susceptible to creep rupture due to softening associated with the increase in water content by dilation and swelling.

8. Although stress relaxation has been less studied than creep, it appears that equally regular patterns of deformation behavior are observed; e.g., (Larcerda and Houston, 1973).
9. Deformation under sustained stress ordinarily produces an increase in stiffness under the action of subsequent stress increase, as shown schematically in Fig. 3.6. This reflects the time-dependent structural readjustment or "aging" that follows changes in stress state.
10. As shown in Fig. 3.7, the locations of both the virgin compression line and the value of the preconsolidation pressure, σ_p' , determined in the laboratory are influenced by the rate of loading during one dimensional consolidation (Graham et al., 1983; Leroueil, et al., 1985). Thus, estimations of the overconsolidation ratio of clay deposits in the field are dependent on the loading rates and paths used in laboratory tests for determination of the preconsolidation pressure. If it is assumed that the relationship between strain and logarithm of time during compression is linear over the time ranges of interest and that the secondary compression index $C_{\alpha e}$ is constant regardless of load, the rate dependent preconsolidation pressure σ_p' at $\dot{\epsilon}_1$, can be related to the axial strain rate as follows (Silvestri et al, 1986; Soga and Mitchell, 1996; Leroueil and Marques, 1996).

$$\frac{\sigma_p'}{\sigma_{p(ref)}'} = \left(\frac{\dot{\epsilon}}{\dot{\epsilon}_{1(ref)}} \right)^{\frac{C_{\alpha e}}{C_c - C_r}} = \left(\frac{\dot{\epsilon}_1}{\dot{\epsilon}_{1(ref)}} \right)^{\alpha} \quad (3.1)$$

where C_c is the virgin compression index, C_r is the recompression index and $\sigma_{p(ref)}'$ is the preconsolidation pressure at a reference strain rate $\dot{\epsilon}_{1(ref)}$. In this equation, the rate effect increases with the value of $\alpha = C_{\alpha e}/(C_c - C_r)$. The variation of preconsolidation pressure with strain rate is shown in Fig. 3.8 (Soga and Mitchell, 1996). The data define straight lines, and the slope of the lines gives the parameter α . In general, the value of α ranges between 0.011 and 0.094. Leroueil and Marques (1996) report values between 0.029 and 0.059 for inorganic clays.

11. The undrained strength of saturated clay increases with increase in rate of strain, as shown in Figs. 3.9 and 3.10. The magnitude of the effect is about 10 percent for each order of magnitude increase in the strain rate. The strain rate effect is considerably smaller for sands. In a manner similar to equation (3.1), a rate parameter β can be defined as the slope of a log-log plot of deviator stress at failure q_f at a particular strain rate $\dot{\epsilon}_1$ relative to $q_{f(ref)}$, the strength at a reference strain rate $\dot{\epsilon}_{1(ref)}$, vs strain rate. This gives the following equation.

$$\frac{q_f}{q_{f(ref)}} = \left(\frac{\dot{\epsilon}_1}{\dot{\epsilon}_{1(ref)}} \right)^\beta \quad (3.2)$$

The value of β ranges between 0.018 and 0.087, similar to the α rate parameter values used to define the rate effect on consolidation pressure in equation (3.1). Higher values of β are associated with more metastable soil structures (Soga and Mitchell, 1996). Rate dependency decreases with increasing sample disturbance, which is consistent with this finding.

3-3 Time Dependent Deformation – Structure Interaction

Time dependent process of particle rearrangement

Creep can lead to rearrangement of particles into more stable configurations. Forces at interparticle contacts have both normal and tangential components, even if the macroscopic applied stress is isotropic. If, during the creep process, there is an increase in the proportion of applied deviator stress that is carried by interparticle normal forces relative to interparticle tangential forces, then the creep rate will decrease. Hence, the rate occurs need not be uniform owing to the particulate nature of soils. Instead it will reflect a series of structural readjustments as particles move up, over, and around each other, thus leading to the somewhat irregular sequence of data points shown in Fig. 3.11.

Microscopically, creep is likely to occur in the weak clusters discussed in Lecture 2 because the contacts in them are at limiting frictional equilibrium. Any small perturbation in applied load at the contacts or time dependent loss in material strength can lead to sliding or yield at asperities. As particles slip, propped strong force network columns are disturbed, and these buckle via particle rolling as discussed Lecture 2 note.

To examine the effects of particle rearrangement, Kuhn (1987) developed a discrete element model that considers sliding at interparticle contacts to be visco-frictional. The rate at which sliding of two particles relative to each other occurs depends on the ratio of shear to normal force at their contact. The relationship between rate and force is formulated in terms of rate process theory (Mitchell and Soga, 2005), and the mechanistic representations of the contact normal and shear forces are shown in Fig. 3.12. The time-dependent component in the tangential forces model is given as a “sinh-dashpot”. The average magnitudes of both normal and tangential forces at individual contacts can change during deformation even though the applied boundary stresses are constant. Small changes in the tangential and normal force ratio at a contact can have a very large influence on the sliding rate at that contact. These changes, when summed over all contacts in the shear zone, result in a decrease or increase in the overall creep rate.

A numerical analysis of an irregular packing of circular disks using the “sinh-dashpot” representation gives creep behavior comparable to that of many soils as shown in Fig. 3.13 (Kuhn and Mitchell, 1993). The creep rate slows if the average ratio of tangential to normal force decreases; whereas, it accelerates and may ultimately lead to failure if the ratio increases. In some cases, the structural changes that are responsible for the decreasing strain rate and increased stiffness may cause the overall soil structure to become more metastable. Then, after the strain reaches some limiting value, the process of contact force transfer from

decreasing tangential to increasing normal force reverses. This marks the onset of creep rupture as the structure begins to collapse. A similar result was obtained by Rothenburg (1992) who performed discrete element analyses, in which smooth elliptical particles were cemented with a model exhibiting viscous characteristics in both normal and tangential directions.

Particle breakage during creep

Particle breakage can contribute to time dependent deformation of sands (Leung et al., 1996; Takei et al., 2001; McDowell, 2003). Leung et al. (1996) performed one-dimensional compression tests on sands, and Fig. 3.14 shows the particle size distribution curves for samples before loading and after two different load durations. The amount of particle breakage increased with load duration. Microscopic observations revealed that angular protrusions of the grains were ground off, producing fines. The fines fill the voids between larger particles and crushed particles progressively rearranged themselves with time.

Aging - Time-dependent strengthening of soil structure

The structural changes that occur during creep that is continuing at a decreasing rate cause an increase in soil stiffness when the soil is subjected to further stress increase as shown in Fig. 3.6. Leonards and Altschaeffl (1964) showed that this increase in preconsolidation pressure cannot be accounted for in terms of the void ratio decrease during the sustained compression period. Time-dependent changes of these types are a consequence of “aging” effects which alter the structural state of the soil. The fabric obtained by creep may be different from that caused by increase in stress, even though both samples arrive at the same void ratio. Leroueil et al. (1996) report a similar result for an artificially sedimented clay from Quebec, as shown in Fig. 3.15(a). They also measured the shear wave velocities after different times during the tests using bender elements and computed the small strain elastic shear modulus. Fig. 3.15(b) shows the change in shear modulus with void ratio.

Additional insight into the structural changes accompanying the aging of clays is provided by the results of studies by Anderson and Stokoe (1978) and Nakagawa et al. (1995). Fig. 3.16 shows changes in shear modulus with time under a constant confining pressure for kaolinite clay during consolidation (Anderson and Stokoe, 1978). Two distinct phases of shear modulus-time response are evident. During primary consolidation, values of the shear modulus increase rapidly at the beginning and begin to level off as the excess pore pressure dissipates. After the end of primary consolidation, the modulus increases linearly with the logarithm of time during secondary compression.

The expected change in shear modulus due to void ratio change during secondary compression can be estimated using the following empirical formula for shear modulus as a function of void ratio and confining pressure (Hardin and Black, 1968).

$$G = A \frac{(2.97 - e)^2}{1 + e} p'^{0.5} \quad (3.3)$$

where A is a material constant, e is the void ratio and p' is the mean effective stress. The dashed line in Fig. 3.16 shows the calculated increases in the shear modulus due to void ratio decrease using equation (3.3). It is evident that the change in void ratio alone does not provide an explanation for the secondary time-dependent increase in shear modulus. This aging effect has been recorded for a variety of materials, ranging from clean sands to natural clays (Afifi

and Richart, 1973; Kokusho, 1987; Mesri et al., 1990 and many others). Further discussion of aging phenomena is given later on.

Time dependent changes in soil fabric

Changes in soil fabric with time under stress influence the stability of soil structure. Changes in sand fabric with time after load application in one dimensional compression were measured by Bowman and Soga (2003). Resin was used to fix sand particles after various loading times. Pluviation of the sand produced a horizontal preferred particle orientation of soil grains, and increased vertical loading resulted in a greater orientation of particle long axes parallel to the horizontal, which is in agreement with the findings of Oda (1972), Mitchell, et al. (1976), and Jang and Frost (1998). Over time, however, the loading of sand caused particle long axes to rotate toward the vertical direction (i.e. more isotropic fabric).

Experimental evidence (Bowman and Soga, 2003) showed that large voids became larger, whereas small voids became smaller, and particles group or cluster together with time. Based on these particulate level findings, it appears that the movements of particles lead to interlocking zones of greater local density. The interlocked state may be regarded as the final state of any one particle under a particular applied load, due to kinematic restraint. The result, with time, is a stiffer, more efficient, load bearing structure, with areas of relatively large voids and neighboring areas of tightly-packed particles. The increase in stiffness is achieved by shear connections obtained by the clustering. Then, when load is applied, the increased stiffness and strength of the granular structure provides greater resistance to the load and the observed “aging” effect is seen. The numerical analysis in Kuhn and Mitchell (1993) led to a similar hypothesis for how a more ‘braced’ structure develops with time. For load application in a direction different to that during the aging period, however, the strengthening effect of aging may be less, as the load bearing particle column direction differs from the load direction.

3-4 Sand Ageing Effects and Their Significance

Over geological time, lithification and chemical reactions can change sand into sandstone or clay into mudstone or shale. However, even over engineering time, behavior of soils can alter as stresses redistribute after construction (Fookes et al., 1998). It is well-established that fine-grained soils and clays have properties and behavior that change over time as a result of consolidation, shear, swelling, chemical and biological changes, etc. Until recently it has not been appreciated that cohesionless soils exhibit this behavior as well. Much recent field evidence of the changing properties of granular soils over time is now available and these data suggest that recently disturbed or deposited granular soils gain stiffness and strength over time at constant effective stress – a phenomenon called ‘aging’. The evidence includes the time-dependent increase in stiffness and strength of densified sands as measured by cone penetration resistance (Mitchell and Solymer, 1984 ; Thomann and Hryciw, 1992; Ng et al., 1998) and the set-up of displacement piles in granular materials (Astedt et al., 1992; York et al., 1994; Chow et al., 1998; Axelsson, 2000; Jardine and Standing, 2000). Hypotheses to explain this phenomenon include both creep processes and chemical and biological cementation processes.

Increase in shear modulus with time

As discussed in Section 3-3, the shear modulus at small strain is known to increase with time under a confining stress, and this is considered to be the consequence of aging. This behavior

can be quantified by a coefficient of shear modulus increase with time using the following formula (Anderson and Stokoe, 1978).

$$I_G = \Delta G / \log(t_2 / t_1) \quad (3.4)$$

$$N_G = I_G / G_{1000} \quad (3.5)$$

where I_G is the coefficient of shear modulus increase with time, t_1 is a reference time after primary consolidation, t_2 is some time of interest thereafter, ΔG is the change in small strain shear modulus from t_1 to t_2 , G_{1000} is the shear modulus measured after 1000 minutes of constant confining pressure, which must be after completion of primary consolidation, and N_G is the normalized shear modulus increase with time. Large increase in stiffness due to aging is represented by large values of I_G or N_G . In general, the measured N_G value for clays ranges between 0.05 and 0.25. The aging effect also increases with an increasing plasticity index as shown in Fig. 3.17 (Kokusho, 1987). The data in the figure have been supplemented by values of $\Delta G/G$ for several sands compiled by Jamiolkowski (1994). Mesri et al. (1990) report that N_G for sands varies between 0.01 and 0.03 and increases as the soil becomes finer. Jamiolkowski and Manassero (1995) give values of 0.01 to 0.03 for silica sands, 0.039 for sand with 50% mica and 0.05-0.12 for carbonate sand. Experimental results show that the rate of increase in stiffness with time for very loose carbonate sand increases as the stress level increases (Howie et al., 2002). Isotropic stress state resulted in a slower rate of increase in stiffness.

There is only limited field data that shows evidence of aging effects on stiffness. Troncoso and Garces (2000) measured shear wave velocities using downhole wave propagation tests in low plasticity silts with fines contents from 50 to 99 percent at four abandoned tailing dams in Chile. The shear modulus normalized by the vertical effective stress is plotted against the age of the deposit in Fig. 3.18. The age of the deposits is expressed as the time since deposition. Although the soil properties vary to some degree at the four sites¹, very significant increase in stiffness at small strains can be observed after 10 to 40 years of aging. The degree to which secondary compression could have contributed to this increase is not known.

Time-dependent behavior after ground improvement

Stiffness and strength of sand increase with time after disturbance and densification by mechanical processes such as blasting and vibrocompaction. Up to 50 percent or more increase in strength has been observed over 6 months (Mitchell and Solymer, 1984; Thomann and Hryciw, 1992; Charlie et al., 1992; Ng et al., 1998; Ashford, et al., 2004) as measured by cone penetration testing.

The Jebba Dam project on the Niger River, Nigeria, was an early well documented field case where aging effects in sands were both significant and widespread (Mitchell and Solymer, 1984). The project involved the treatment of foundation soils beneath a 42 m high dam and seepage blanket. Due to large depths of the loose sand deposit requiring

¹ The four sites identified by Troncoso and Garces (2000) are called Barahona, Cauquenes, La Cocinera and Veta del Agua and the aging times between abandonment and testing were 28, 19, 5 and 2 years, respectively. The tailing deposits at Barahona had a liquid limit of 41% and a plastic limit of 14%, whereas those at other three sites had liquid limits of 23-29% and plastic limits of 2-6%.

densification, a two stage densification program was performed. The upper 25 m of sand (and a 5 to 10 m thick sand pad placed by hydraulic filling of the river) was densified using vibrocompaction. Deposits between depths of 25 to 40 m were densified by deep blasting.

During the blasting operations, it was observed that the sand exhibited both sensitivity; i.e. strength loss on disturbance, and aging effects. A typical example of the initial decrease in penetration resistance after blasting densification and subsequent increase with time is shown in Fig. 3.19. Initially after improvement, there was in some cases a decrease in penetration resistance, despite the fact that surface settlements ranging from 0.3 to 1.1 m were measured. With time (measured up to 124 days after improvement), however, the cone penetration resistance was found to increase by approximately 50-100% of the original values. Similar behavior was found following blast densification of hydraulic fill sand that had been placed for construction of Treasure Island in San Francisco Bay more than 60 years previously (Ashford et al., 2004).

Aging effects were also observed after placement of hydraulic fill working platforms in the river at the Jebba Dam site and after densification by vibrocompaction as shown in Figs. 3.20 and 3.21. In the case of vibrocompaction, however, there was considerable variability in the magnitude of aging effects throughout the site. Because of the greater density increase caused by vibrocompaction than by blast densification, no initial decrease in the penetration resistance was observed at the end of the compaction process.

Charlie et al. (1992) found a greater rate of aging after densification by blasting for sands in hotter climates than in cooler climates and suggested a correlation between the rate of aging and mean annual air temperature for available field data as shown in Fig. 3.22. In the figure, the increase in the CPT tip resistance (q_c) with time is expressed by the following equation.

$$\frac{q_c(N \text{ weeks})}{q_c(1 \text{ week})} = 1 + K \log N \quad (3.6)$$

where N is the number of weeks since disturbance and K expresses the rate of increase in tip resistance in logarithmic time.

Schmertmann (1991) postulated that ‘complicated soil structure’ is present in freshly deposited soil. The structure then becomes more stable by ‘drained dispersive movements’ of soil particles. He suggests that stresses would arch from softer, weaker areas to stiffer zones with time, leading to an increase in K_0 with time. Mitchell and Solymar (1984) suggested that the cementation of particles may be the mechanism of aging of sands, similar to diagenesis in locked sands and young rocks (Dusseault and Morgenstern, 1979; Barton, 1993) in which grain overgrowth has been observed. However, others have questioned whether significant chemical reactions can occur over the short time of observations. In addition, there is some evidence of aging in dry sands wherein chemical processes would be anticipated to be very slow.

Set-up of displacement piles

Much field data indicates that the load carrying capacity of a pile driven into sand may increase dramatically over several months, long after pore pressures have dissipated (e.g., Chow et al., 1998; Jardine and Standing, 2000). The amount of increase is highly variable, ranging from 20% to 170% per log cycle of time as shown in Fig. 3.23 (Chow et al., 1998;

Bowman, 2003). Most of the increase in capacity occurs along the shaft of the pile as the radial stress at rest increases with time (Axelsson, 2000). Evidence suggests that piles in silts and fine sands set up more than those in coarse sands and gravels (York et al., 1994). Both driven and jacked piles exhibit set up, whereas bored piles do not. Hence, the stress-strain state achieved during the construction processes of pile driving have an influence on this time dependent behavior and various mechanisms have been suggested to explain this (Astedt et al., 1992; Chow et al., 1998; Axelsson, 2002; Bowman, 2003). Unfortunately, at present, there is no conclusive evidence to confirm any of the proposed hypotheses.

Despite the many field examples and laboratory studies on aging effects, there is still uncertainty about the mechanism(s) responsible for the phenomenon. Understanding the mechanism(s) that cause aging is of direct practical importance in the design and evaluation of ground improvement, driven pile capacity, and stability problems where strength and deformation properties and their potential changes with time are important. Mechanical, chemical and biological factors have been hypothesized for the cause of aging. Biological processes have so far been little studied; however mechanical and chemical phenomena have been investigated in more detail, and some current understanding is summarized below.

3-5 Mechanical Processes of Aging

Creep is hypothesized as the dominant mechanism of aging of granular systems on an engineering time-scale by Mesri et al. (1990) and Schmertmann (1991). Increased strength and stiffness does not occur solely from the change in density that occurs during secondary compression. Rather, it is due to a continued rearrangement of particles resulting in increased macro-interlocking of particles and increased micro-interlocking of surface roughness. This is supported by the existence of locked sands (Barton, 1993; Richards and Barton, 1999), which exhibit a tensile strength even without the presence of binding cement.

Although no increase in stiffness was detected when glass balls were loaded isotropically (Losert et al., 2000), sand has been found to increase in strength and stiffness under isotropic stress conditions (Daramola, 1980; Human, 1992). These increases develop even under isotropic confinement because the angular particles can lock together in an anisotropic fabric. It has been shown that more angular particles produce materials more susceptible to creep deformations (Mejia et al., 1988, Human, 1992, Leung et al., 1996). Isotropic compression tests by Kuwano (1999) showed that radial creep strains were greater than axial strains in soils with angular particles than in soils with rounded particles due to a more anisotropic initial fabric. Angular particles can result in longer duration of creep and a greater aging effect since they have a larger range of stable contacts and the particles can interlock. As spherical particles rearrange more easily than elongated ones (Oda, 1972), rounder particles initially creep at a higher rate before settling into a stable state. Hence, any aging effect on rounded particles tends to disappear quickly when the soil is subjected to new stress state.

When a constant shear stress is applied to loose sand, large creep accompanied by volumetric contraction is observed (Bopp and Lade, 1997). Higher contact forces due to loose assemblies contribute to increased particle crushing, contributing to contraction behavior. Hence, decrease in volume by soil crushing leads to increase in stiffness and strength.

Field data suggest that displacement piles in medium-dense to dense sands set up more than those in loose sand (York et al., 1994). Dense granular materials may dilate with time depending on the applied stress level during creep as shown in Fig. 3.24 (Bowman and Soga, 2003). Initially, the soil contracts with time, but then at some point the creep vector rotates and the dilation follows. Similar observations were made by Murayama et al. (1984) and Lade and Lui (1998). This implies that sands at a high relative density will set up more as more interlock between particles may occur (Bowman, 2003). The laboratory observation of initial contraction followed by dilation conveniently explains the field data of dynamic compaction where the greater initial losses and eventual gains in stiffness and strength of sands are found close to the point of application where larger shear stresses are applied to give dilation (Dowding and Hryciw, 1986; Thomann and Hryciw, 1992; Charlie et al., 1992).

Increased strength and stiffness due to mechanical aging occurs predominantly in the direction of previously applied stress during creep (Howie et al., 2001). No increase was observed when the sand was loaded in a direction orthogonal to that of the applied shear stress during creep (Losert et al., 2000).

3-6 Chemical Processes of Aging

Chemical processes are a possible cause of aging. Historically, the most widespread theory used to explain aging effects in sand has involved interparticle bonding. Terzaghi originally referred to a “bond strength” in connection with the presence of a quasi-preconsolidation pressure in the field (Schmertman, 1992). Generally, this mechanism has been thought of as type of cementation, which would increase the cohesion of a soil without affecting its friction angle.

Denisov and Reltov (1961) showed that quartz sand grains adhered to a glass plate over time. They placed individual sand grains on a vibrating quartz or glass plate and measured the force necessary to move the grains as shown in Figure 3.25. The dry grains were allowed to sit on the plate for varying times and then the plate was submerged, also for varying times, before vibrating began. It was found that the force required to move the sand grains continued to increase up to about 15 days of immersion in water. The cementating agent was thought to be silica-acid gel, which has an amorphous structure and would form a precipitate at particle contacts (Mitchell and Solymar, 1984). The increased strength is derived from crystal overgrowths caused by pressure solution and compaction.

Strong evidence of a chemical mechanism being responsible for some aging was obtained by Joshi et al. (1995). A laboratory study was made of the effect of time on penetration resistance of specimens prepared with different sands (river sand and sea sand) and pore fluid compositions (air, distilled water and sea water). After loading under a vertical stress of 100 kPa, the values of penetration resistance were obtained after different times up to two years. Strength and stiffness increases were observed in all cases, and a typical plot of load-displacement curves at various times is shown in Fig. 3.26. The effects of aging were greater for the submerged sand than for the dry specimens. Scanning electron micrographs of the aged specimens in distilled water and sea water showed precipitates on and in between sand grains. For the river sand in distilled water, the precipitates were composed of calcium (the soluble fraction of the sand) and possibly silica. For the river sand in sea water, the precipitates were composed of sodium chloride.

However, there are several reported cases in which cementation was an unlikely mechanism of aging, at least in the short-term. For example, dry granular soils can show an increase in stiffness and strength with time (Human, 1992; Joshi et al., 1995; Losert et al., 2000). Cementation in dry sand is unlikely, as moisture is required to drive solution and precipitation reactions involving silica or other cementation agents.

Mesri et al. (1990) used the triaxial test data from Daramola (1980) to argue against a chemical mechanism responsible for aging effects in sands. Fig. 3.27 shows the effects of aging on both the stiffness and shear strength of Ham River sand. Four consolidated drained triaxial tests were performed on samples with the same relative density and confining pressure (400 kPa), but consolidated for different periods of time (0, 10, 30 and 152 days) prior to the start of the triaxial tests. The results showed that the stiffness increased and the strain to failure decreased with increasing time of consolidation. Although increased values of modulus were observed, the strain at failure is approximately 3%. Mesri et al. (1990) argue that this large strain would destroy any cementation, and therefore another less brittle mechanism must be responsible for the increase in stiffness.

In summary, experimental evidence indicates that mechanical aging behavior is enhanced by shear stress application and in denser materials. It is also associated with the micro-interlocking occurring during the generation of creep strain. The increase in stiffness and strength is observed in the direction of the applied stresses, but the aging effect disappears rather quickly when loads are applied in other directions. Chemical aging can also occur within days depending on such factors as chemical environment and temperature.

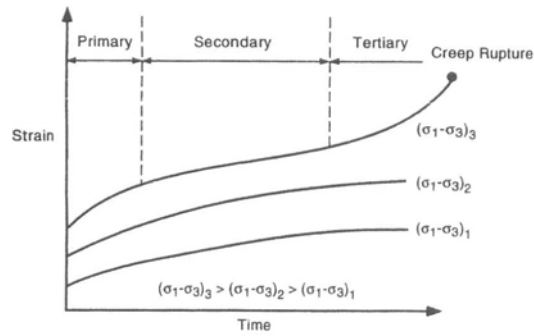
Some conditions in natural deposits are not replicated in small-scale laboratory testing. Most laboratory tests are done using clean granular materials; whereas, in the field there will be impurities, biological activity, and heterogeneity of void ratio and fabric. Furthermore, the introduction of air and other gases during ground improvement may have consequences that have so far not been fully evaluated. Arching associated with dissipation of blast gases and the redistribution of stresses through the soil skeleton may also play a role (Baxter and Mitchell, 2004). The boundary conditions associated with penetration testing in rigid wall cylinders in the laboratory may prevent detection of time-dependent increases in penetration resistance that are measured under the free-field conditions in the field.

3-7 Summary

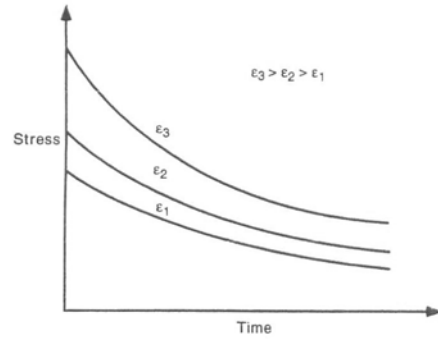
With exception of settlement rate predictions, most soil mechanics analyses used in geotechnical engineering assume limit equilibrium and are based on the assumption of time-independent properties and deformations. In reality, time-dependent deformations and stress changes that result from the time-dependent or viscous rearrangement of the soil structure may be responsible for a significant part of the total ground response.

Recognition of the fact that any macroscopic stress applied to a soil mass induces both tangential and normal forces at the interparticle contacts is essential to the understanding of rheological behavior. The results of discrete element analyses show that changes in creep rate with time can be explained by changes in the tangential and normal force ratio at interparticle contacts that result from particle rearrangement during deformation. The change in microfabric in relation to strong particle networks and weak clusters leads to possible explanation of the mechanical aging process.

Time-dependent deformations and stress relaxation follow predictable patterns that are essentially the same for all soil types. Simple constitutive equations can reasonably describe time-dependent behavior under limited conditions. Much remains to be learned, however, about the influences of combined stress states, stress history and transient drainage conditions on creep, stress relaxation, and creep rupture before reliable analyses and predictions can be made for large and complex geotechnical structures.



(a)



(b)

Fig. 3-1

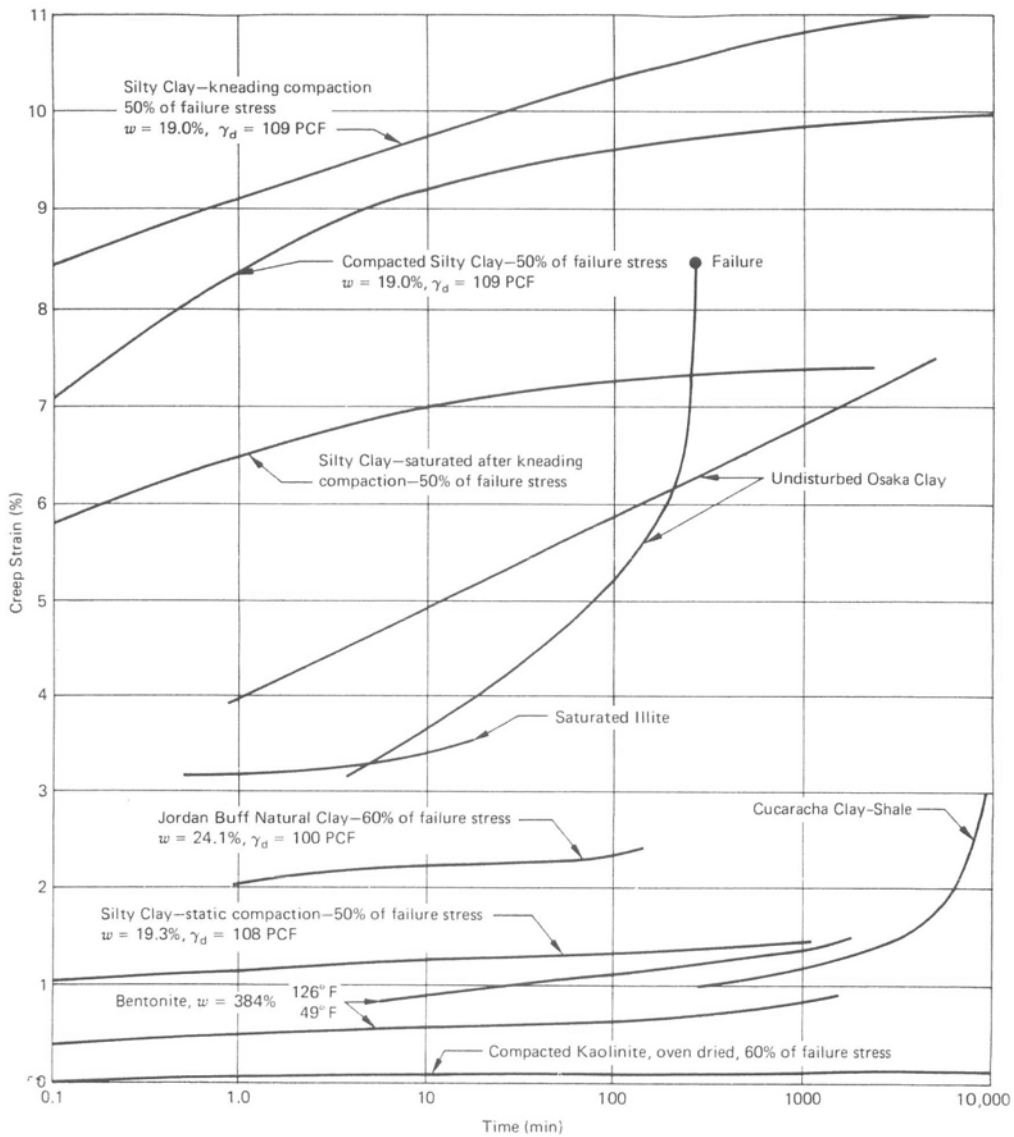


Fig. 3-2

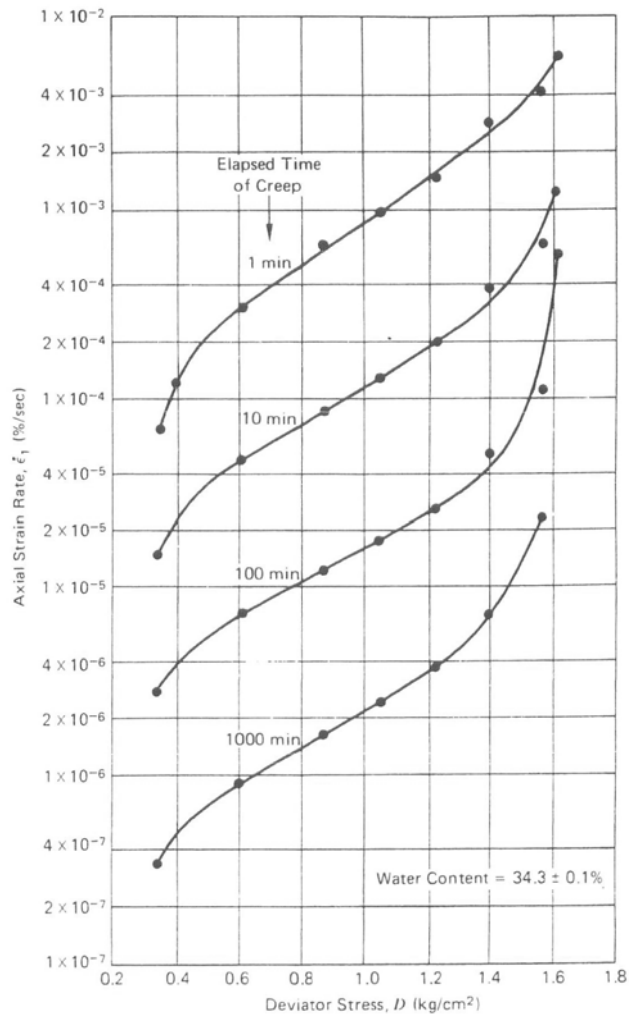


Fig. 3-3

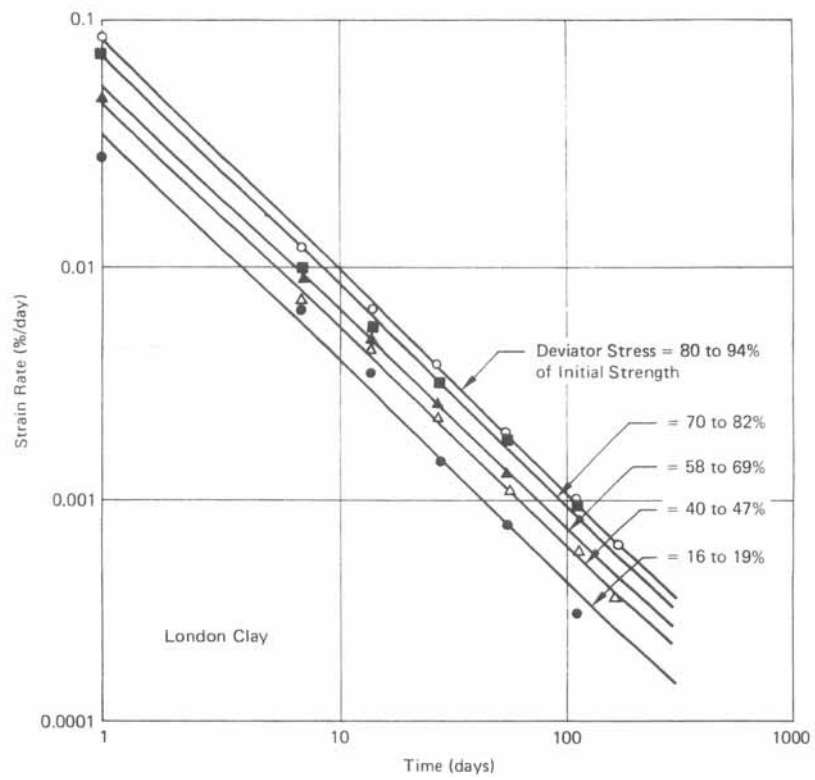


Fig. 3-4

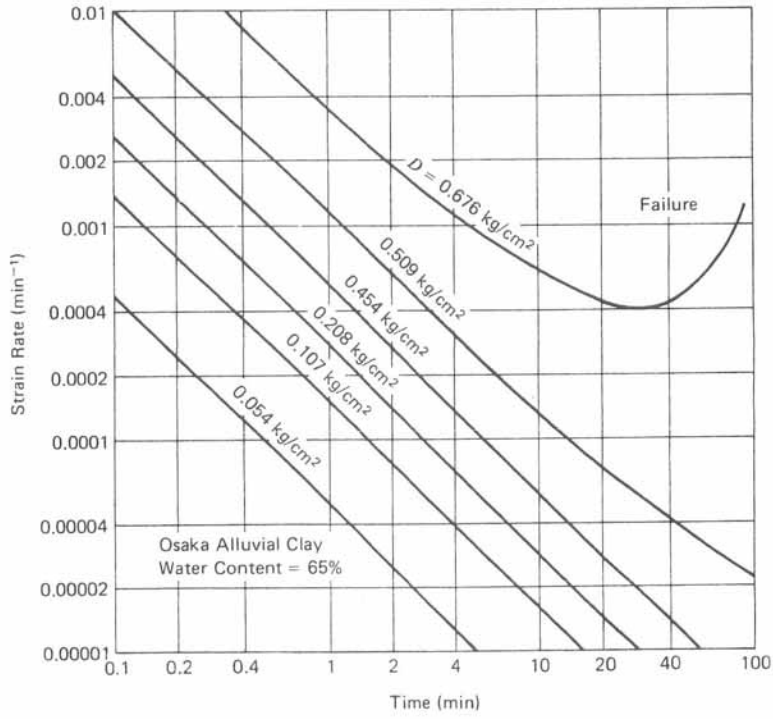


Fig. 3-5

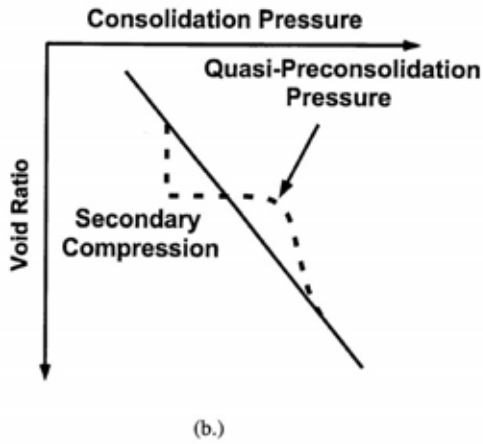
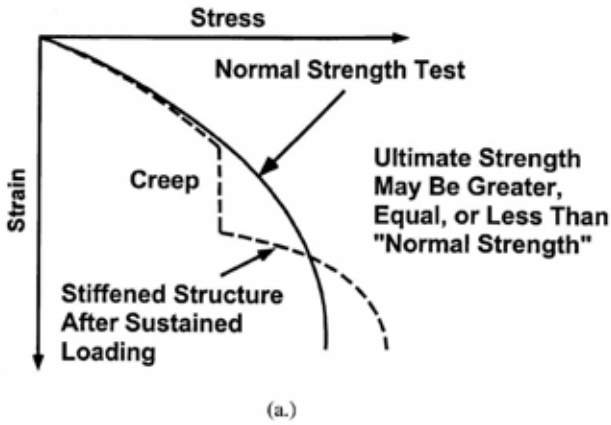


Fig. 3-6

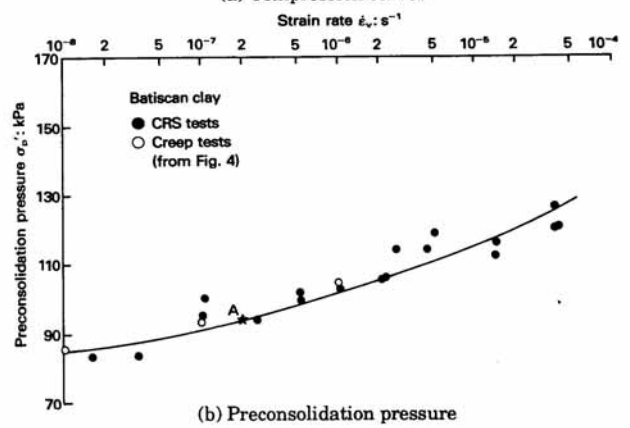
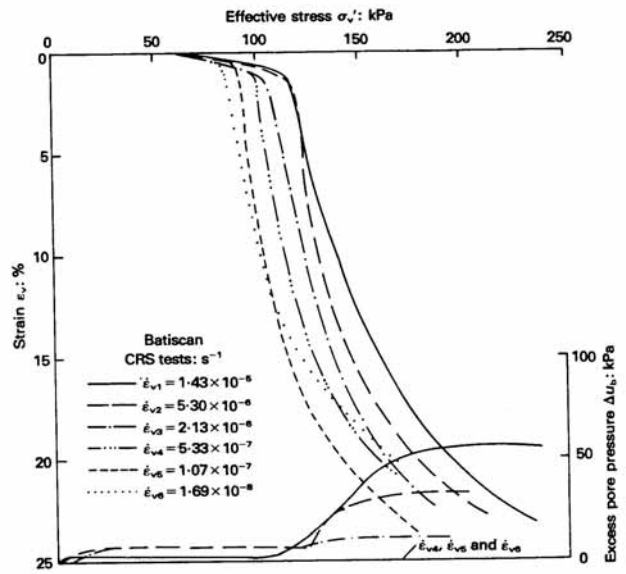


Fig. 3-7

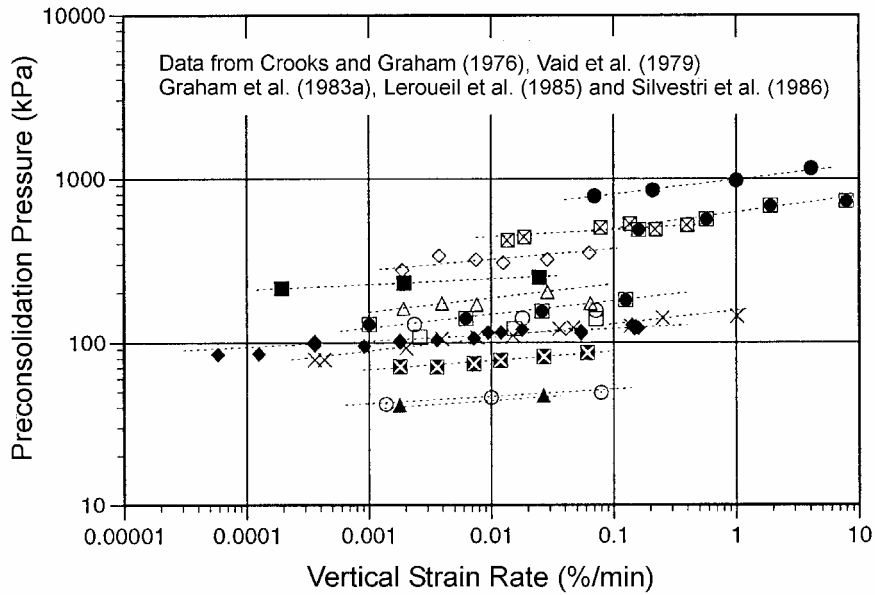


Fig. 3-8

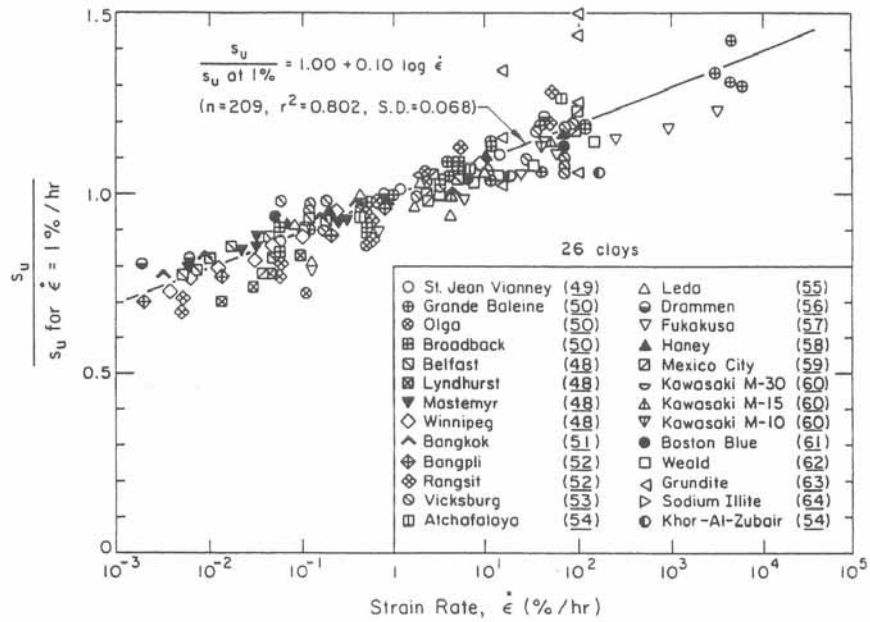


Fig. 3-9

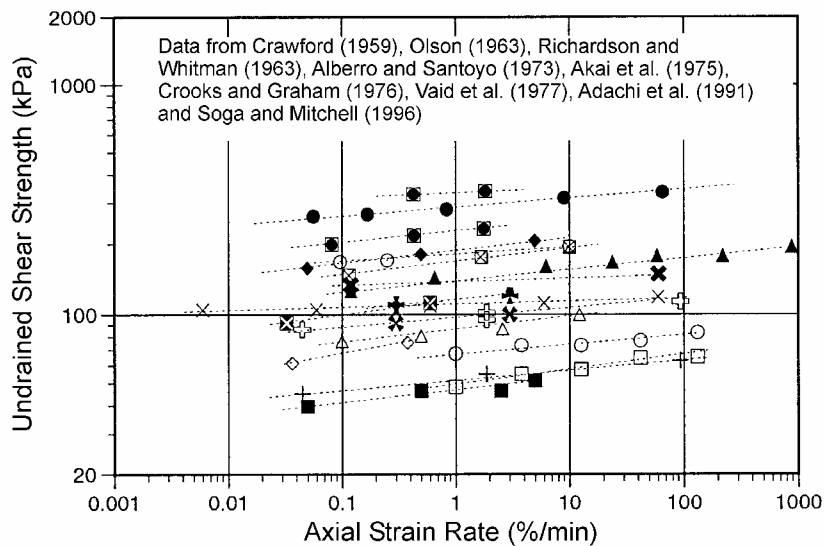


Fig. 3-10

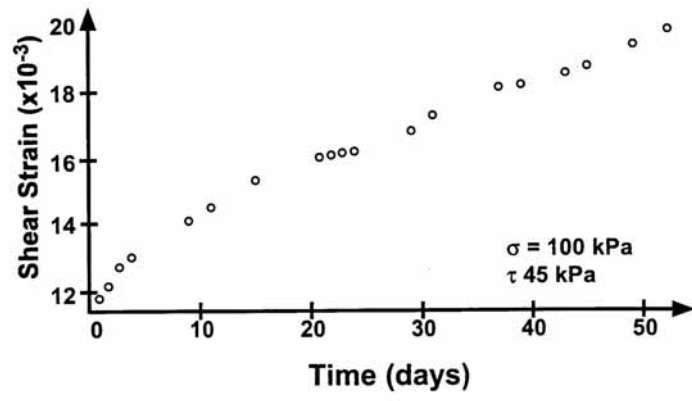


Fig. 3-11

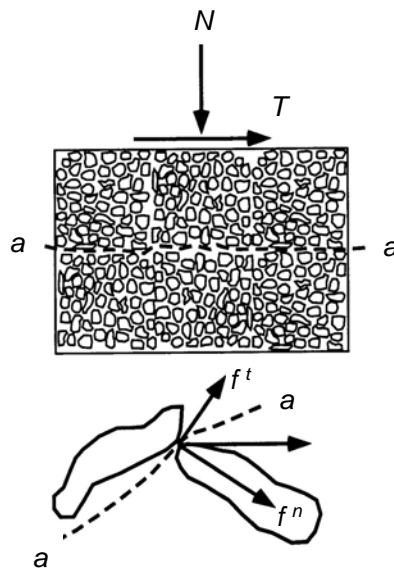
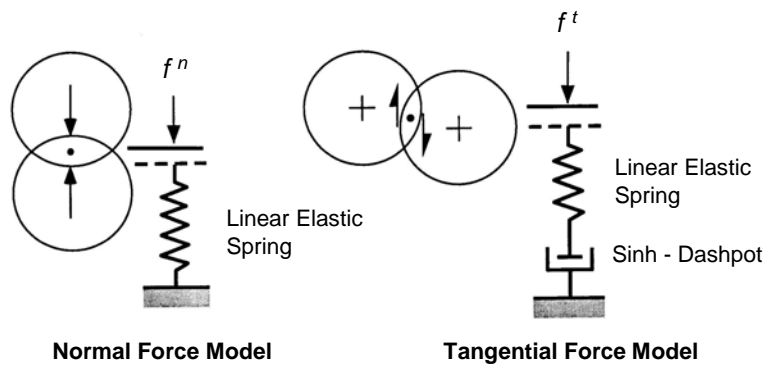


Fig. 3-12

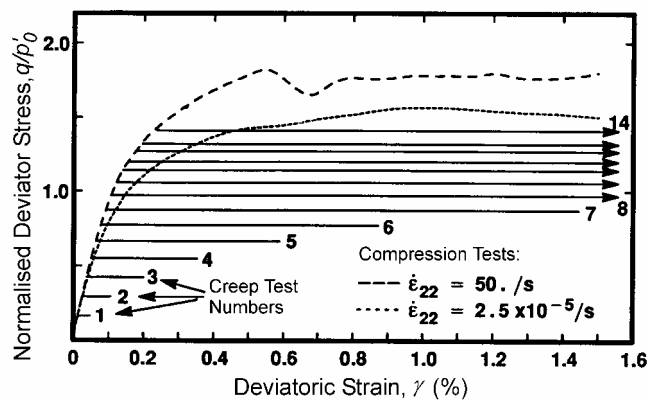


Fig. 3-13a

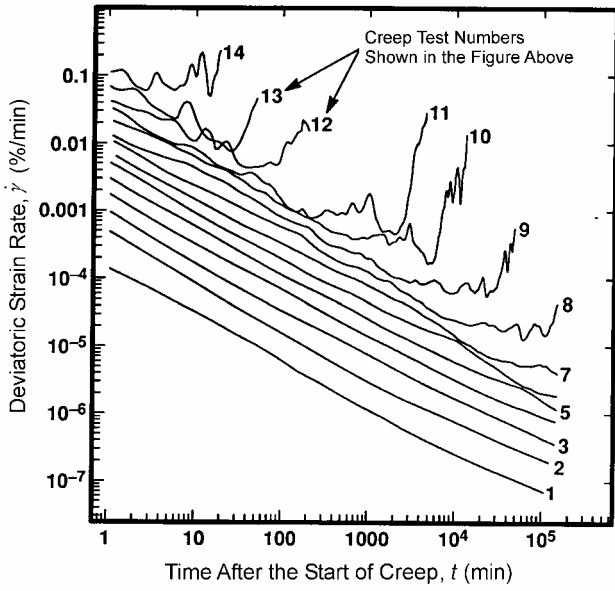


Fig. 3-13b

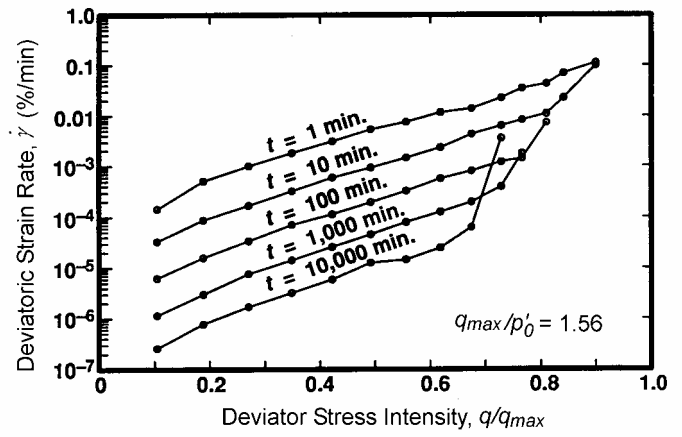


Fig. 3-13c

Fig. 15. Particle size distribution of sand.

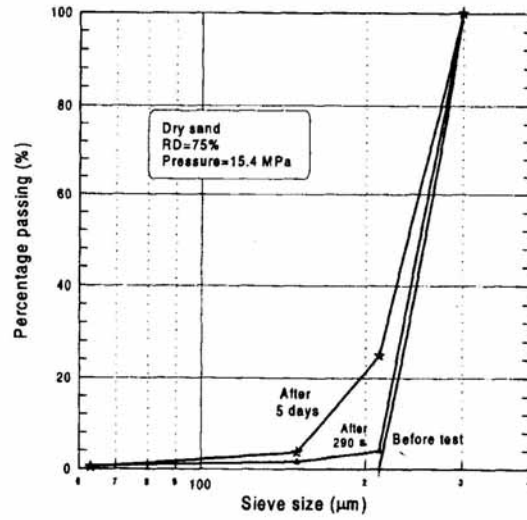


Fig. 3-14

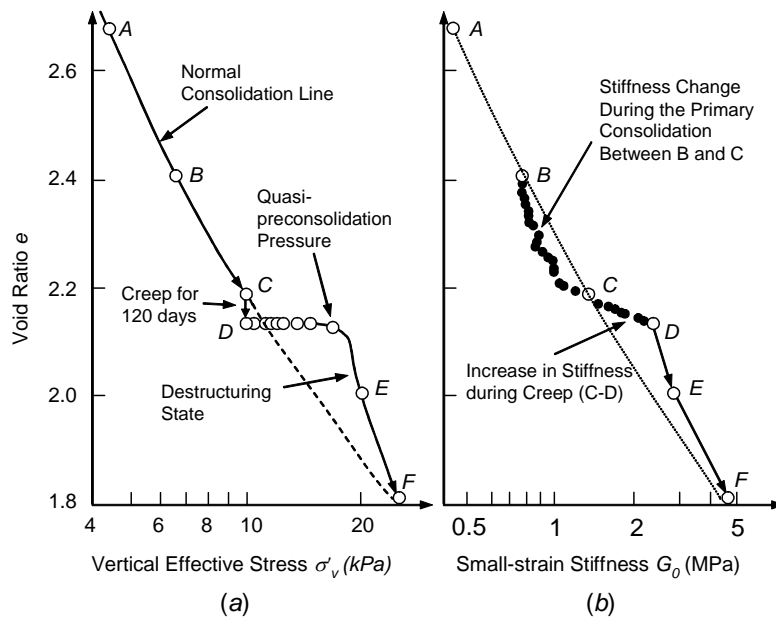


Fig. 3-15

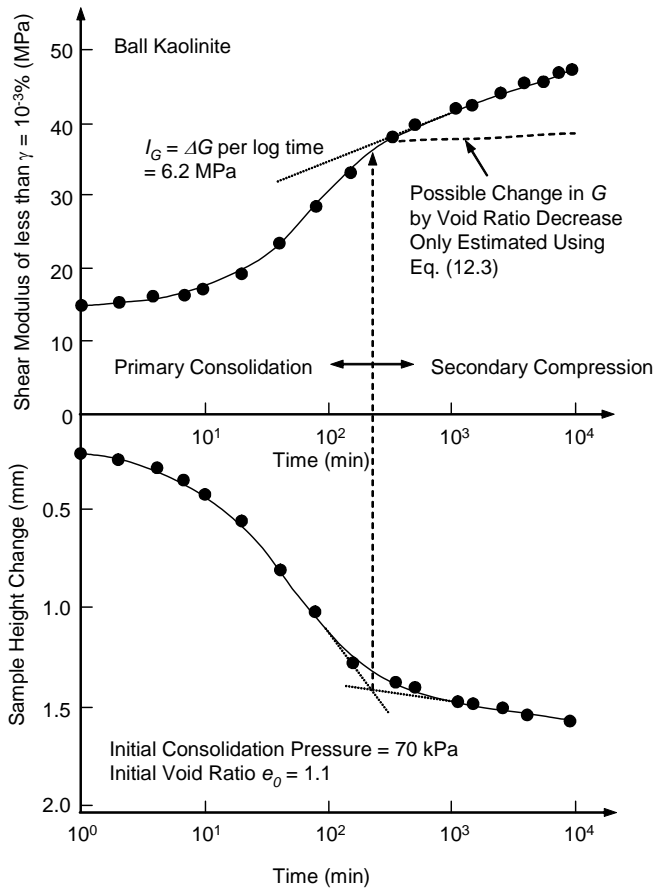


Fig. 3-16

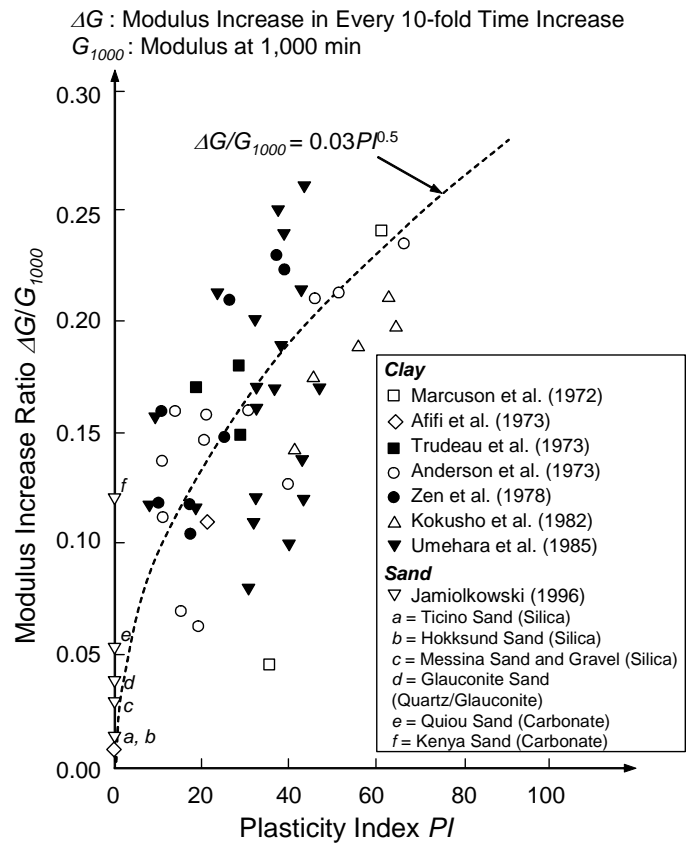


Fig. 3-17

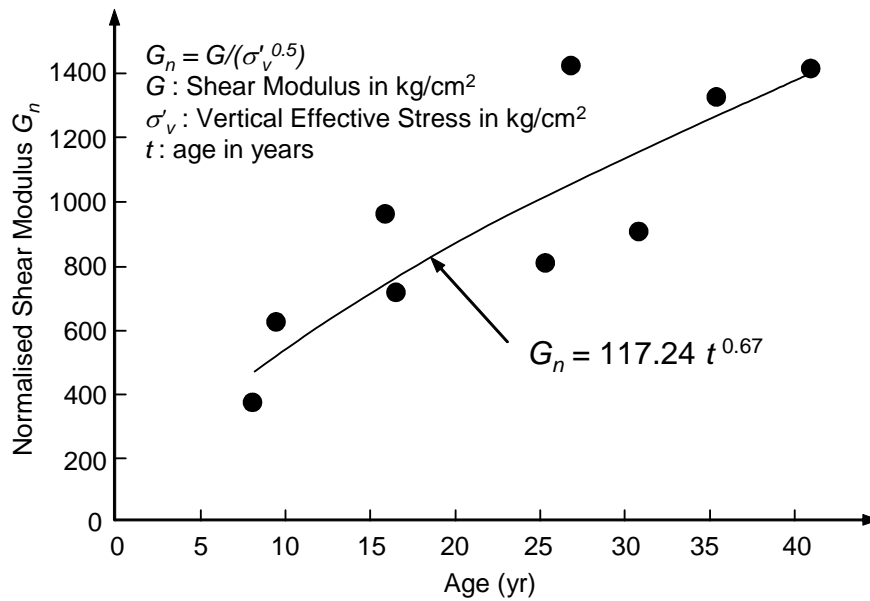


Fig. 3-18

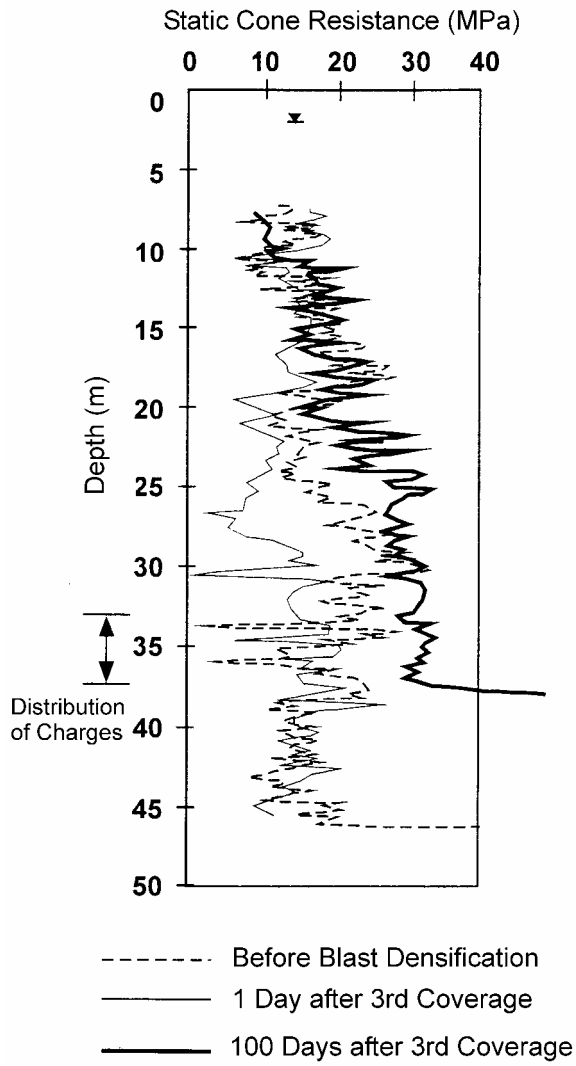


Fig. 3-19

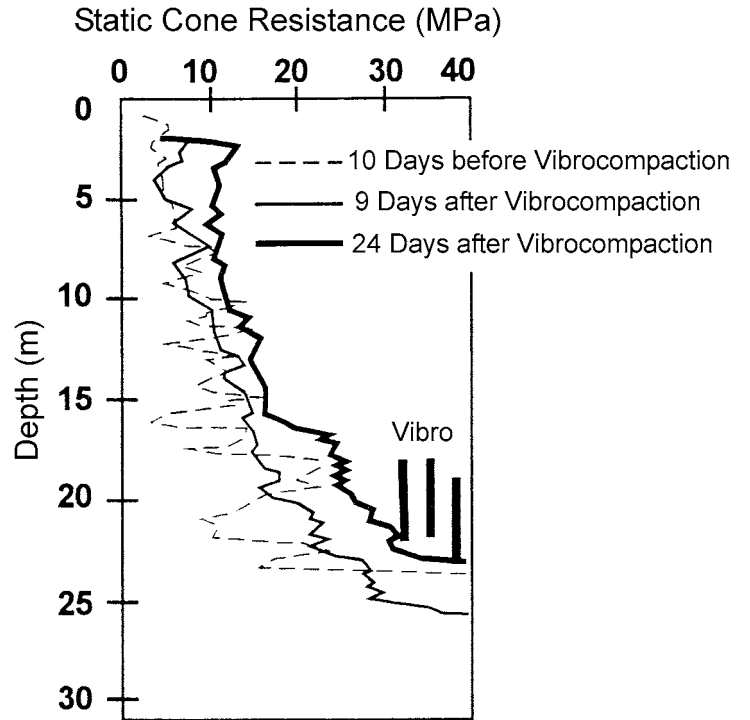


Fig. 3-20

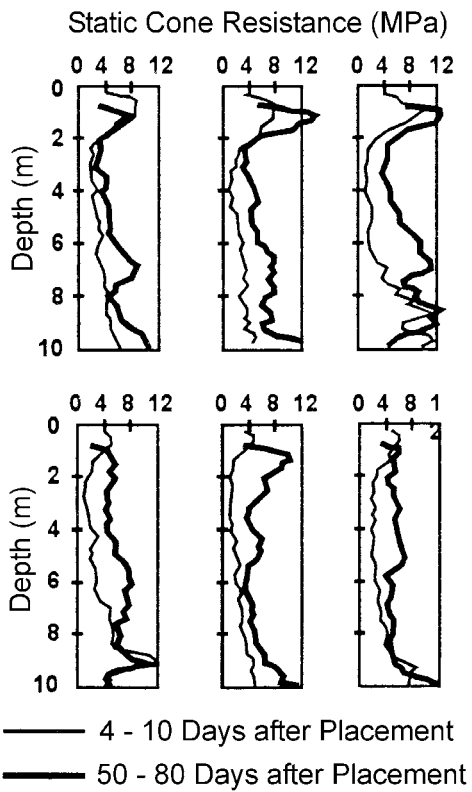


Fig. 3-21

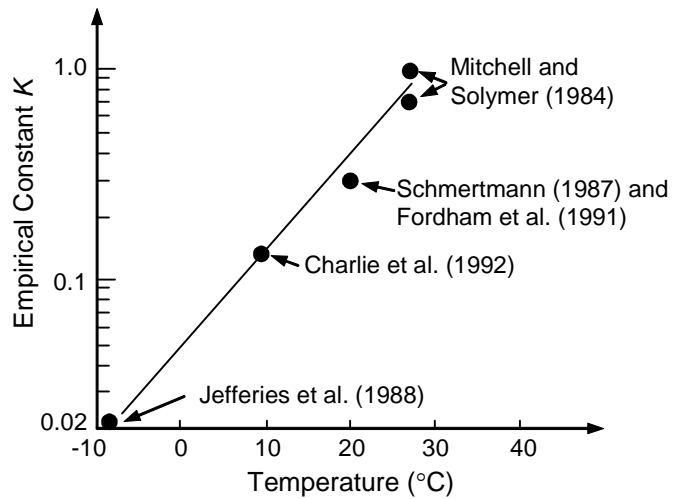
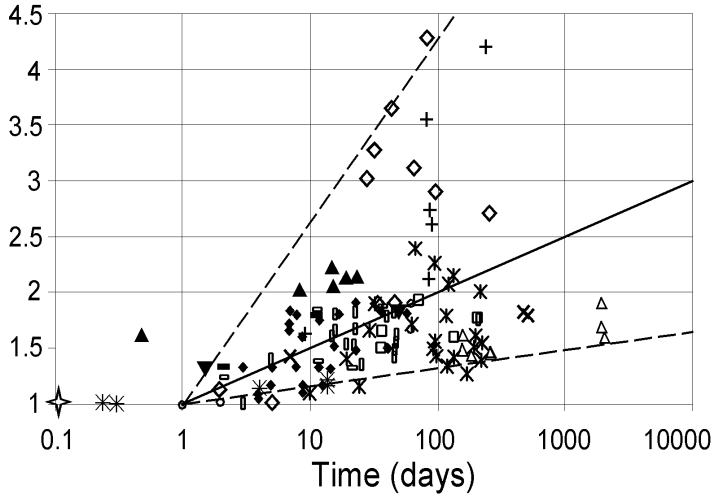


Fig. 3-22

Pile Capacity Increase Q_t/Q_{t0}



Shaft Capacity Increase Q_s/Q_{s0}

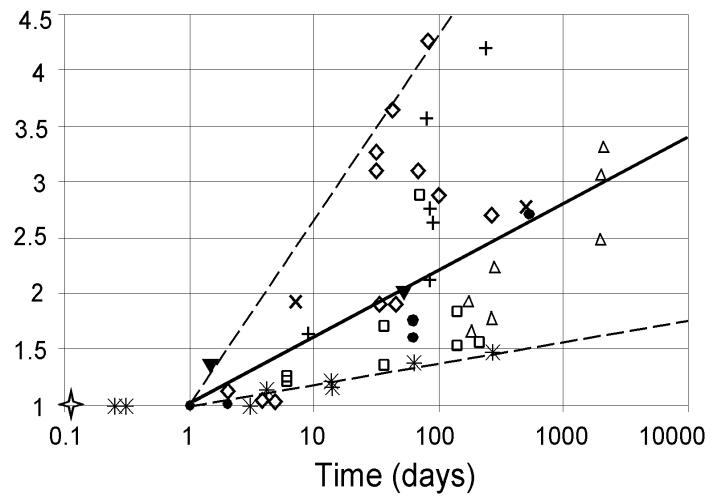


Fig. 3-23

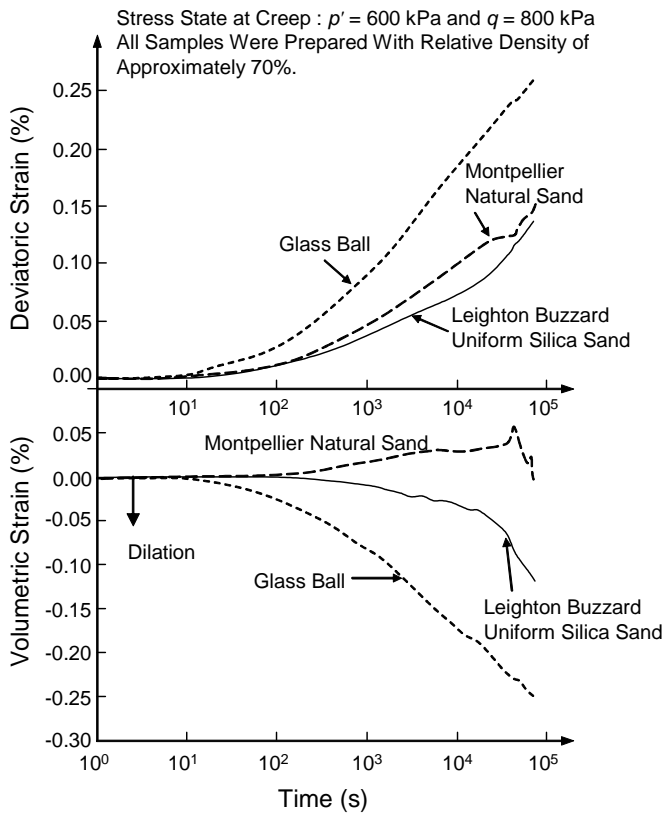


Fig. 3-24

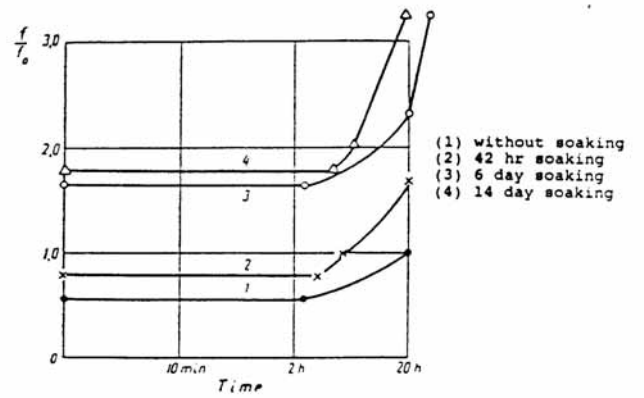
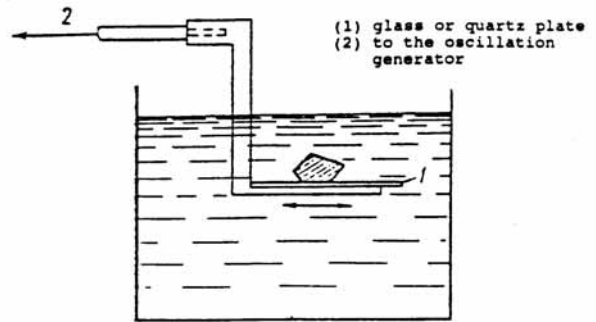


Fig. 3-25

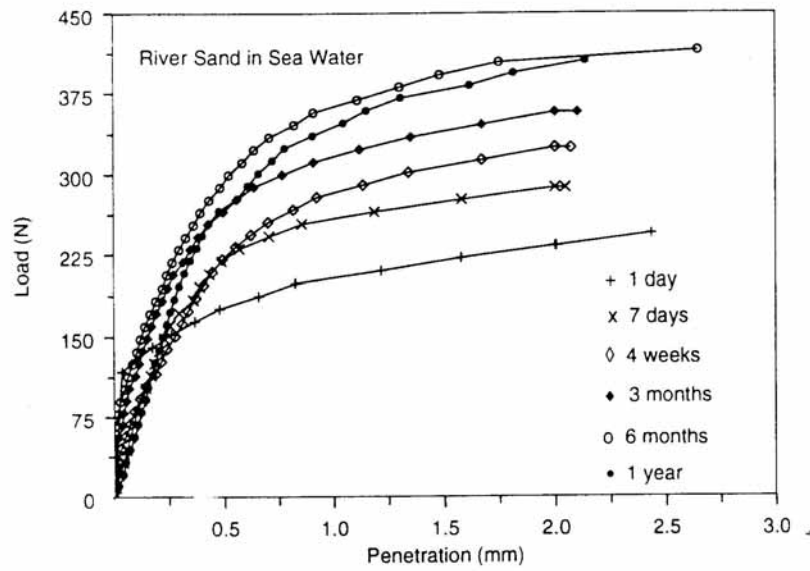


Fig. 3-26

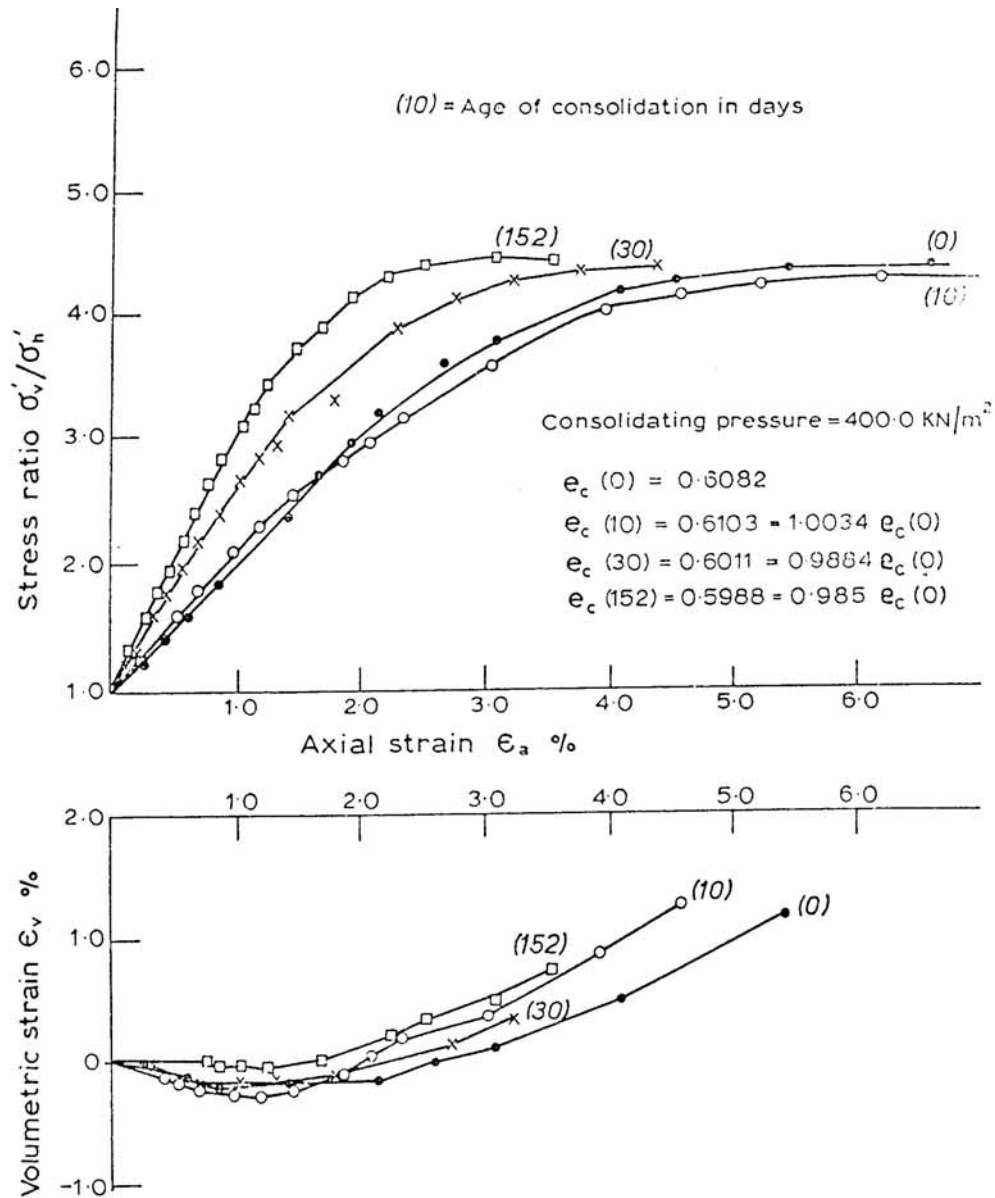


Fig. 3-27